

# Immunotoxicity evaluation of novel bioactive composites in male mice as promising orthopaedic implants

GEHAN T. EL-BASSYOUNI<sup>1</sup>, MARIAM G. ESHAK<sup>2</sup>, IBRAHIM A.H. BARAKAT<sup>2,3</sup>, WAGDY K.B. KHALIL<sup>2</sup>

<sup>1</sup>Biomaterials Department, National Research Centre, Cairo, Egypt

<sup>2</sup>Cell Biology Department, National Research Centre, Giza, Egypt

<sup>3</sup>Zoology Department, College of Science, King Saud University, Riyadh, Saudi Arabia

## Abstract

**Objective:** In orthopaedics, novel bioactive composites are largely needed to improve the synthetic achievement of the implants. In this work, semiconducting metal oxides such as SiO<sub>2</sub>, TiO<sub>2</sub>, and ZrO<sub>2</sub> particles (Ps) were used individually and in different ratios to obtain different biphasic composites. The immunotoxicity of these composites was tested to inspect the potential toxicity prior to their use in further medical applications.

**Materials and methods:** In vitro mineralisation ability was inspected by soaking the composites in simulated body fluid (SBF). Additionally, in vivo experiments were performed consuming male mice using ISSR-PCR, micronucleus (MN) test, comet assay, glutathione peroxidase activity, and determination of albumin, globulin, lymphocyte population, ALT, and AST levels. Several groups of adult male albino mice were treated with 100, 200, and 400 mg/kg body weight of SiO<sub>2</sub>, TiO<sub>2</sub>, and ZrO<sub>2</sub>-Ps in pure or mixed forms.

**Results:** Our findings revealed that treatment of mice with low and medium doses of SiO<sub>2</sub>, TiO<sub>2</sub>, and ZrO<sub>2</sub>-Ps in pure or mixed form revealed values relatively similar to the control group. However, using 400 mg/kg especially from TiO<sub>2</sub>-Ps in genuine form or mixed with SiO<sub>2</sub> showed proliferation in the toxicity rates compared with the high dose of SiO<sub>2</sub> and ZrO<sub>2</sub>-Ps.

**Conclusions:** The results suggest that TiO<sub>2</sub> composite induced in vivo toxicity, oxidative DNA damage, bargain of the antioxidant enzymes, and variations in the levels of albumin, globulin, lymphocyte population, ALT, and AST in a dose-dependent manner. However, SiO<sub>2</sub> and ZrO<sub>2</sub> composites revealed a lower toxicity in mice compared with that of TiO<sub>2</sub>.

**Key words:** semiconducting metal oxides, ISSR-PCR, DNA damage, MN formation, glutathione peroxidase activity, A/G ratio, lymphocyte population.

(Cent Eur J Immunol 2017; 42 (1): 54-67)

## Introduction

Some bioactive ceramics have already been used to repair bone defects due to their bioactivity, which allows them to achieve tight fixation resulting from direct bonding to living bone. The first bioactive ceramic developed was a glass in the Na<sub>2</sub>O-CaO-SiO<sub>2</sub>-P<sub>2</sub>O<sub>5</sub> system, after Hench [1]. This bioactive glass was named Bioglass. Many researchers have established various types of bioactive ceramics [2-5]. They have lower fracture toughness and higher Young's modulus than that of human cortical bone [6]. Therefore, the development of novel bioactive materials with amended mechanical and biological properties, in addition to high affinity for bone tissue, was looked for.

It is important for ceramic materials to form a bone-like apatite layer on their surfaces after being exposed to

the body environment, to speed their property of direct bonding to living bone. A similar bone-like apatite layer can be formed on bioactive ceramics, if they were immersed in a simulated body fluid (SBF), as proposed by Kokubo *et al.* SBF is an aqueous solution that has almost the same ingredients, with regard to the inorganic species, as human extracellular fluid [7-10]. Simulated body fluid does not contain any cells or proteins, which means that the apatite layer is formed through the chemical reaction of the bioactive ceramics with the surrounding fluid. It is therefore anticipated that novel bioactive materials can be produced by controlling the chemical reactivity of the materials in body fluid [11].

Based on this idea, new types of bioactive materials, such as composites of (amorphous silica) SiO<sub>2</sub> strengthened with either (titania) TiO<sub>2</sub> or (zirconia) ZrO<sub>2</sub>, have been developed.

However, titania powder with high surface area are not easily obtained due to their phase transformation and crystallite growth. Therefore, efforts have been directed towards the preparation of SiO<sub>2</sub>/TiO<sub>2</sub> composite microspheres in order to hinder the phase transformation [12]. Moreover, SiO<sub>2</sub>/TiO<sub>2</sub> composite microspheres may exhibit novel properties that are not found in a single oxide. It was reported that SiO<sub>2</sub>/TiO<sub>2</sub> composite exhibited superior catalytic properties to the classical oxides and less biocompatibility than titania and silica [13].

Titania (TiO<sub>2</sub>), as a naturally occurring oxide, is a talented material. It possesses suitable mechanical and biocompatible properties [14, 15]. TiO<sub>2</sub> can initiate the formation of a strong bond to bone upon implantation via the formation of a hydroxyapatite [Ca<sub>10</sub>(PO<sub>4</sub>)<sub>6</sub>(OH)<sub>2</sub>, HA] layer [16]. Furthermore, it was found that TiO<sub>2</sub> in SiO<sub>2</sub>/TiO<sub>2</sub> composite microspheres demonstrated better photoactivity than pure TiO<sub>2</sub> particles due to their smaller grain size and improved absorption [17].

Zirconia (ZrO<sub>2</sub>) and titanium were used extensively in dental and orthopaedic implantation because of their mechanical properties and chemical resistance to degradation by bodily fluids. ZrO<sub>2</sub> is tough because of its tetragonal structure; this structure can be controlled by blending it with other materials in order to balance toughness and strength. It is also one of the most extensively used ceramics in medical fields due to its good biocompatibility, excellent corrosion resistance, high strength, and low cost [18, 19]. There is interest in using ZrO<sub>2</sub> for biomedical applications in high load-bearing sites [20]. The biological inertness and the good biocompatibility of ZrO<sub>2</sub> have been confirmed by many medical applications [21]. Zirconia has been commonly used in orthopaedic implant materials offering better [22] scratch resistance relative to metal and better resistance to brittle fracture than alumina (Al<sub>2</sub>O<sub>3</sub>) [22-25]. In 2002, Uchida *et al.* found that the Zr-OH group formed on zirconium metal after pre heat treatment in ≥ 5 M aqueous sodium hydroxide (NaOH) solution showed the ability to induce apatite formation in simulated body fluid SBF [26-28].

To date, there has been no published data available concerning evaluation of the *in vivo* toxicity of SiO<sub>2</sub>, TiO<sub>2</sub>, and ZrO<sub>2</sub> composites. Therefore, the present study was planned to explore the bio-safety of novel bioactive composites of SiO<sub>2</sub>, TiO<sub>2</sub>, and ZrO<sub>2</sub> on the immune and genetic materials of male mice before its use in further biomedical applications.

## Material and methods

### Chemicals

TiO<sub>2</sub> powder (anatase form) was purchased from BDH (England). Silicon oxide (SiO<sub>2</sub>), amorphous, 99.5%, was purchased from Alfa Aesar (USA). Zirconia powder (Zirconium Oxide, ZrO<sub>2</sub>) was purchased from Zircoa (Germany). The chemicals for molecular analysis (ISSR-PCR) were bought from Invitrogen (Carlsbad, CA, USA).

### *In vitro* bioactivity test

Results obtained from *in vitro* experiments cannot usually be restructured as is to expect the reaction of an entire organism *in vivo*. Building a reliable extrapolation procedure from *in vitro* results to *in vivo* is therefore essential. The importance of exploring *in vitro* bioactivity prior to *in vivo* is quite clear, as *in vivo* studies require animal sacrifices, which are more costly, less easily reproducible, and involve ethical issues. For these reasons, before *in vivo*, screenings being carried out in *in vitro* tests are necessary. The scientific community hypothesised that SBF can be used to assess the *in vitro* bioactivity of a material. Simulated body fluid is an aprotic and acellular solution that has an inorganic ion concentration similar to that of human extracellular fluid, to mimic the formation of apatite on bioactive materials *in vitro*.

To study the bioactivity, samples were soaked in 50 ml of simulated body fluid (SBF) with ion concentrations (Na<sup>+</sup> 142.0, K<sup>+</sup> 5.0, Mg<sup>2+</sup> 1.5, Ca<sup>2+</sup> 2.5, Cl<sup>-</sup> 147.8, HCO<sub>3</sub><sup>-</sup> 4.2, HPO<sub>4</sub><sup>2-</sup> 1.0, SO<sub>4</sub><sup>2-</sup> 0.5 Mm) nearly equal to those of human blood plasma at 36.5°C. Simulated body fluid (prepared following Kokubo's protocol) [7, 8]. Simulated body fluid was prepared by dissolving reagent grade chemicals one by one in the order NaCl, NaHCO<sub>3</sub>, KCl, K<sub>2</sub>HPO<sub>4</sub>·3H<sub>2</sub>O, MgCl<sub>2</sub>·6H<sub>2</sub>O, CaCl<sub>2</sub>, and Na<sub>2</sub>SO<sub>4</sub> into double-distilled water, and buffered at pH 7.40 with tris(hydroxymethyl)aminomethane [(CH<sub>2</sub>OH)CNH<sub>3</sub>] and approximately 45 mM of hydrochloric acid (HCl) at 36.5°C. After soaking for 15 days, samples were withdrawn from the SBF solution, gently washed with distilled water, dried in air, and kept in an incubator to assess their acellular bioactivity [29, 30].

To estimate the formation of hydroxycarbonate apatite (HCA) aggregates on the surface of materials post immersion, samples were characterised via scanning electron microscopy (SEM, JEOL JXA-840, Tokyo, Japan, Electron Probe Micro-analyser).

### *In vivo* study

**Experimental animals:** The animal experiments were conducted at the animal house facility, affiliated to the National Research Centre (NRC). The study *in vivo* protocol was approved by the Institutional Animal Ethics Committee of the NRC. Two hundred and ninety adult male albino mice (20-25 g, purchased from the Animal House Colony, Giza, Egypt) were maintained on standard laboratory diet (protein, 16.04%; fat, 3.63%; fibre, 4.1%; and metabolic energy, 0.012 MJ) and water *ad libitum*. After an acclimation period of one week, animals were estranged into several groups (10 mice/group) and housed individually in filter-top polycarbonate cages housed in a temperature-controlled (23 ± 1°C) and artificially illuminated (12-hour dark/light cycle) room free from any source of chemical detoxification.

**Experimental design:** According to Najda *et al.* [31], three doses of unmixed and mixed materials of SiO<sub>2</sub>, TiO<sub>2</sub>,

and ZrO<sub>2</sub>-particles (Ps): 100, 200, and 400 mg/kg were used for the evaluation of toxicity. The *in vivo* experiments were performed on negative control (untreated mice), positive control (cyclophosphamide), and the experimental groups including unmixed and mixed materials of SiO<sub>2</sub>, TiO<sub>2</sub>, and ZrO<sub>2</sub>. The experimental groups were divided into three unmixed subgroups (SiO<sub>2</sub>, TiO<sub>2</sub>, and ZrO<sub>2</sub>, respectively) and six mixed subgroups (SiO<sub>2</sub>/TiO<sub>2</sub>: 1 : 1, 1 : 2, and 1 : 3; SiO<sub>2</sub>/ZrO<sub>2</sub>: 1 : 1, 1 : 2, and 1 : 3, respectively). All groups had corresponding numbers of animals per test in which for Inter Simple Sequence Repeats (ISSR), bone marrow micronucleus (MN), and enzyme activity assays, for each dose 10 animals were used. All animals were given an IP single dose once per week for one month. The control group was treated with saline water. A known mutagen, cyclophosphamide, at a dose of 40 mg/kg body weight (bw) was used for the positive control group. It was given intraperitoneally (i.p.), and the volume injected was 0.01 ml/g b.w. Samples of liver were immediately kept on ice and frozen at -20°C prior to usage for ISSR-PCR and enzyme activity analyses. Bone marrow samples were collected from both femurs of each animal and extracted immediately and processed for the MN assay.

**Extraction of genomic DNA:** Total genomic DNA was isolated from mice liver tissue samples (100 mg) by cutting first into very fine pieces and digesting at 37°C overnight in TNES-Urea solution (10 mM Tris-HCl, 125 mM NaCl, 10 mM EDTA 2Na, 1% SDS, and 8 M Urea) with 10 mg/ml proteinase K, as described by Asahida *et al.* [32]. DNA was extracted from each sample following the standard procedure of SDS-phenol chloroform. Subsequently, DNA was precipitated in cold ethanol, re-suspended in TE buffer, and stored at 4°C until PCR amplification. The concentration of genomic DNA samples was determined via UV spectrometer and necessary dilutions were done, followed by verification with 0.8% agarose gel electrophoresis.

**ISSR-PCR and electrophoresis:** Inter Simple Sequence Repeat (ISSR) analysis was performed using the six different primers listed in Table 1. The primers contained different di- and tri-nucleotide repeat motifs in order to achieve as wide as possible genome coverage. For each primer, the annealing temperature was chosen after different trials with different

**Table 1.** ISSR primer codes, sequences, and their annealing temperature used for ISSR-PCR

Primer set	Primer Code	Primer sequence (5'-3')	Annealing T (°C)
1	HB8	(GA) 6 GG	48
2	HB9	(GT) 6 GG	48
3	HB10	(GA) 6 CC	48
4	HB11	(GT) 6 CC	48
5	HB15	(GTG) 3 GC	52
6	814	(CT) 8 TG	44

temperatures (tested range from 48-52°C), aiming to maximise the information obtained from the patterns, i.e. maximum amplification, minimum smear on gels (from non-specific amplification), and well-resolved bands.

The PCR solution (25 µl total volumes) contained 0.5 units of Taq DNA Polymerase (Pharmacia®), 1× reaction buffer, 2.5 mM MgCl<sub>2</sub>, 0.2 µM primer, 200 µM of each dNTP, and up to 30 ng of genomic DNA. PCR amplifications were performed using the following conditions: 94°C for two minutes; 35 cycles of: 94°C for 30 seconds, 44°C for 45 seconds, 72°C for 1 minute 30 seconds; 72°C for 20 minutes; and 4°C soak forever. In order to exclude PCR artefacts and verify the repeatability of the results, negative controls and replicates were included in each PCR amplification. For ISSR marker profiling, PCR products were subjected to electrophoresis on 1.5% agarose gels, followed by staining using ethidium bromide [an intercalating agent commonly used as a fluorescent tag (nucleic acid stain) in molecular biology]. The electrophoretic patterns of the PCR products were digitally recorded using a Gel-Doc 2000 image analysis system (Bio-Rad) according to the instruction of the manufactory.

**Micronucleus test:** Acridine orange [an organic compound used as a nucleic acid-selective fluorescent cationic dye useful for cell cycle determination – being cell-permeable, it interacts with DNA and RNA by intercalation or electrostatic attractions respectively] staining of erythrocytes was performed using a procedure used by Ueda *et al.* [33]. To assess this assay, five animals from each treatment were sacrificed after the exposure period. The bone marrow cells were collected from both femurs and re-suspended in a small volume of foetal calf serum (FBS; Sigma) on a 0.003% acridine orange-coated glass slide. The slide was then covered with a cover glass to prepare bone marrow specimens. Slides were dried overnight and fixed with methanol for 10 minutes. Bone marrow specimens were examined in a blinded manner using fluorescence microscopy at 600× or higher magnification with a blue excitation wavelength (e.g. 488 nm) and yellow-to-orange barrier filter (e.g. 515 nm long pass). Two slides per animal were observed once by a single observer who had sufficient experience of micronucleus test. The number of micronucleated polychromatic erythrocytes (%MnPCEs) was measured at a rate of 3000 polychromatic erythrocytes (PCEs) per animal.

**Comet assay for DNA strand break determination:** Mice hepatic tissues of all groups were subjected to modified single-cell gel electrophoresis [34]. In order to obtain the cells, a small piece of the liver was first thoroughly washed using an excess amount of ice-cold Hank's balanced salt solution (HBSS) and then minced quickly, using a pair of stainless steel scissors, to form approximately 1-mm<sup>3</sup> pieces, while immersed in HBSS. After several washings with cold phosphate-buffered saline to get rid of red blood cells (RBCs), the minced liver was dispersed individually into single cells using a pipette. In brief, the

protocol for electrophoresis involved embedding the isolated cells in agarose gel on microscopic slides, lysing them with detergent at high salt concentrations (overnight in the cold), treatment with alkali to denature the DNA (20 minutes), and electrophoresis under alkaline conditions (30 minutes) at 300 mA, 25 V. After electrophoresis the slides were stained by means of ethidium bromide and examined using a fluorescence microscope (Olympus BX60 F-3) with a green filter at  $\times 40$  magnification. For each experimental condition, about 100 cells (about 25 cells per fish) were examined to determine the percentage of cells with DNA damage, which appear as comet-like shapes. Randomly selected non-overlapping cells were visually assigned a score on an arbitrary scale of 0–3 (i.e. class 0 = no detectable DNA damage and no tail; class 1 = tail with a length less than the diameter of the nucleus; class 2 = tail of length between  $1\times$  and  $2\times$  the nuclear diameter; and class 3 = tail longer than  $2\times$  the diameter of the nucleus), based on apparent comet tail length migration and relative proportion of DNA in the nucleus [35]. A total damage score for each slide was derived by multiplying the number of cells assigned to each class of damage by the numeric value of the class and summing up all the values. Slides were analysed by one observer to minimise the scoring variability.

#### Determination of glutathione peroxidase activity:

Glutathione peroxidase activity measurements were carried out by a procedure according to El-Megeed *et al.* [36]. The reaction mixture consisted of 8 mM  $H_2O_2$ , 40 mM guaiacol, 50 mM sodium acetate buffer pH 5.5, and a suitable amount of the enzyme preparation. Change in absorbance at 470 nm due to guaiacol oxidation was followed at 30-second intervals. One unit of glutathione peroxidase activity was defined as the amount of enzyme that increases the O.D. 1.0/min under standard assay conditions.

**Determination of albumin and globulin as well as A/G ratio levels:** Serum albumin and globulin were assessed according to manufacturer instructions of commercially available test kits.

**Analysis of lymphocyte population in blood:** Lymphocyte population distribution in peripheral blood of male mice in different treated groups was examined using flow cytometry method [37].

**Determination of aspartate aminotransferase (AST) and alanine aminotransferase (ALT):** AST and ALT activities were measured using kits of QCA, Spain, according to the method of Rasmy *et al.* [38]. AST and ALT activities were expressed as U/l.

#### Statistical analysis

All data were analysed using the General Liner Models (GLM) procedure of the Statistical Analysis System [39], followed by Scheffé-test to assess significant differences

between groups. The values are expressed as mean  $\pm$  SEM. All statements of significance were based on a probability of  $p < 0.05$ .

## Results

### Surface morphology

The water molecules found in the SBF instantaneously react with the Si–O–Si or Ti–O–Ti bond to form additional Si–OH or Ti–OH groups (Figs. 1, 2). These formed groups induce the nucleation of apatite, as well as the discharge of both the  $Ca^{2+}$  and  $Na^+$  ions from the SBF solution, which

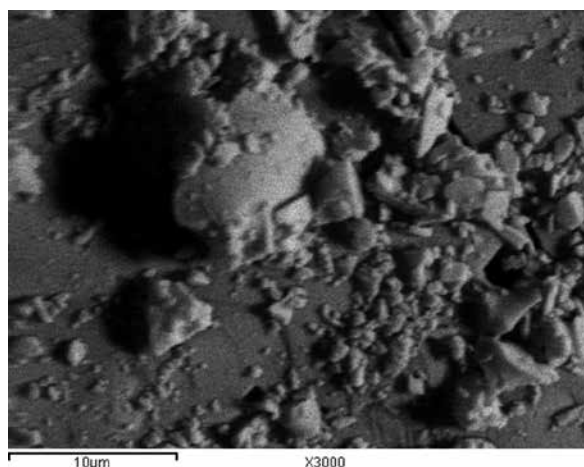


**Fig. 1.** SEM micrograph of pure  $SiO_2$  represents different agglomerates precipitated on top of the sample after immersion for two weeks

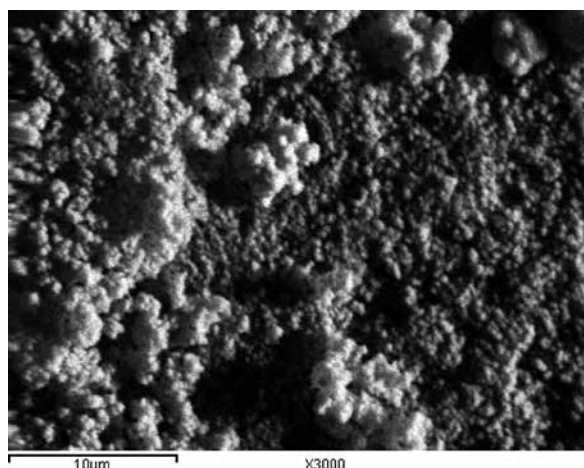


**Fig. 2.** SEM micrograph shows pure  $TiO_2$  with few agglomerates. The image of pure  $TiO_2$  indicates a fairly homogeneous granular surface with fine grain boundaries. The crystals seem to be well-bonded to, and partially embedded in the matrix due to the shadow surrounding the crystals

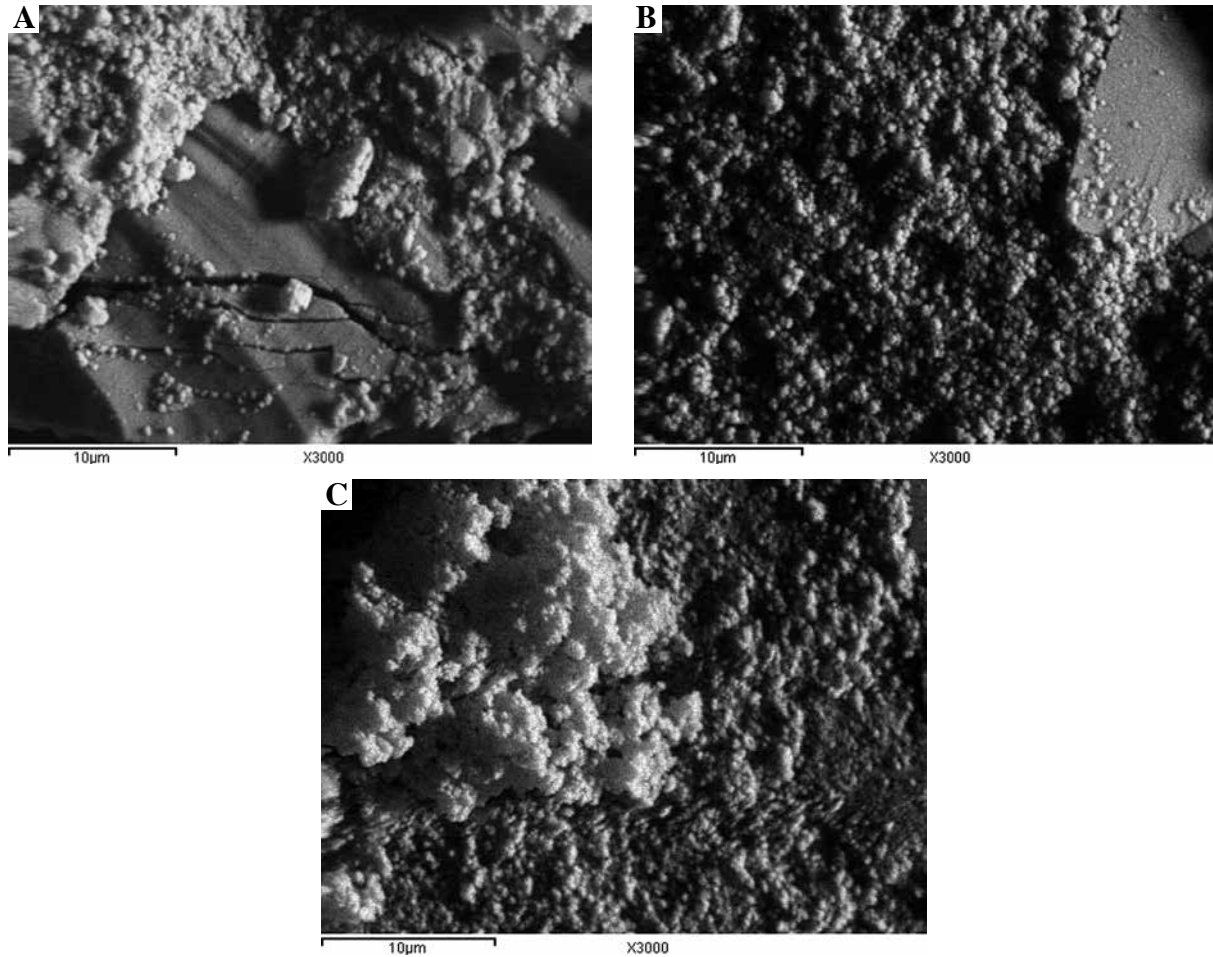


**Fig. 3.** SEM micrograph of  $\text{SiO}_2\text{:TiO}_2$  composite of ratio 1 : 1 (A), 1 : 2 (B), and 1 : 3 (C), respectively

may speed up apatite nucleation by increasing the ionic activity product of the apatite in the fluid. As a result, the apatite layer formed on the composite surface after soaking in SBF was confirmed by SEM of the  $\text{SiO}_2\text{/TiO}_2$  composites post-immersion as shown in Fig. 3. For ratio 1 : 1 composite, SEM at 3000 $\times$  shows that it has many particles on its surface proving slight formation of apatite layer due to the high content of silica in the composite illustrating melted and dense structure that reduced the nucleation of apatite layer compared to other composites. In this domain, the simultaneous dissolution of silicates results in the formation of the silanol (Si-OH) groups on the material's surface, which are crucial as nucleation sites resulting in HA development [40]. Once the apatite nuclei form, they can grow instinctively by overwhelming the calcium phosphate (CaP) ions already found in the surrounding SBF fluid [41]. For biocomposites of ratio 1 : 2 and 1 : 3 the SEM at the same magnification indicates the presence of abundant spherical shapes formed in several layers accumulating over each other to form a bone-like apatite layer for both composites, especially those with the higher content of ti-

tania.  $\text{TiO}_2$  has a propensity to adsorb water at its surface, resulting in the formation of titanium hydroxide (Ti-OH) groups, which were reported to persuade apatite nucleation and crystallisation in SBF [29]. This result may be due to the high content of titania, which leads to an upsurge of Ti-OH groups at the expense of Si-OH groups, resulting in the high nucleation of apatite [42]. The roughness of the surface increases with increasing concentration of  $\text{TiO}_2$  [43]. The thick layer is probably formed due to the large agglomerations of titania particles in these biocomposites (Fig. 3C), which may act as sites for the nucleation and growth of HA [17].

In addition, the results in Fig. 4B–D show the SEM micrograph of  $\text{SiO}_2\text{:ZrO}_2$  composite of ratio 1 : 1, 1 : 2, and 1 : 3 at the same magnification (3000 $\times$ ). The growth of the apatite layer, covering the surface of the zirconia substrate, was very poor. In addition, the smaller groups of a few clustered particles were formed on the substrate as shown in the figures. The coating has an imperfect structure and very low crystallinity [30].

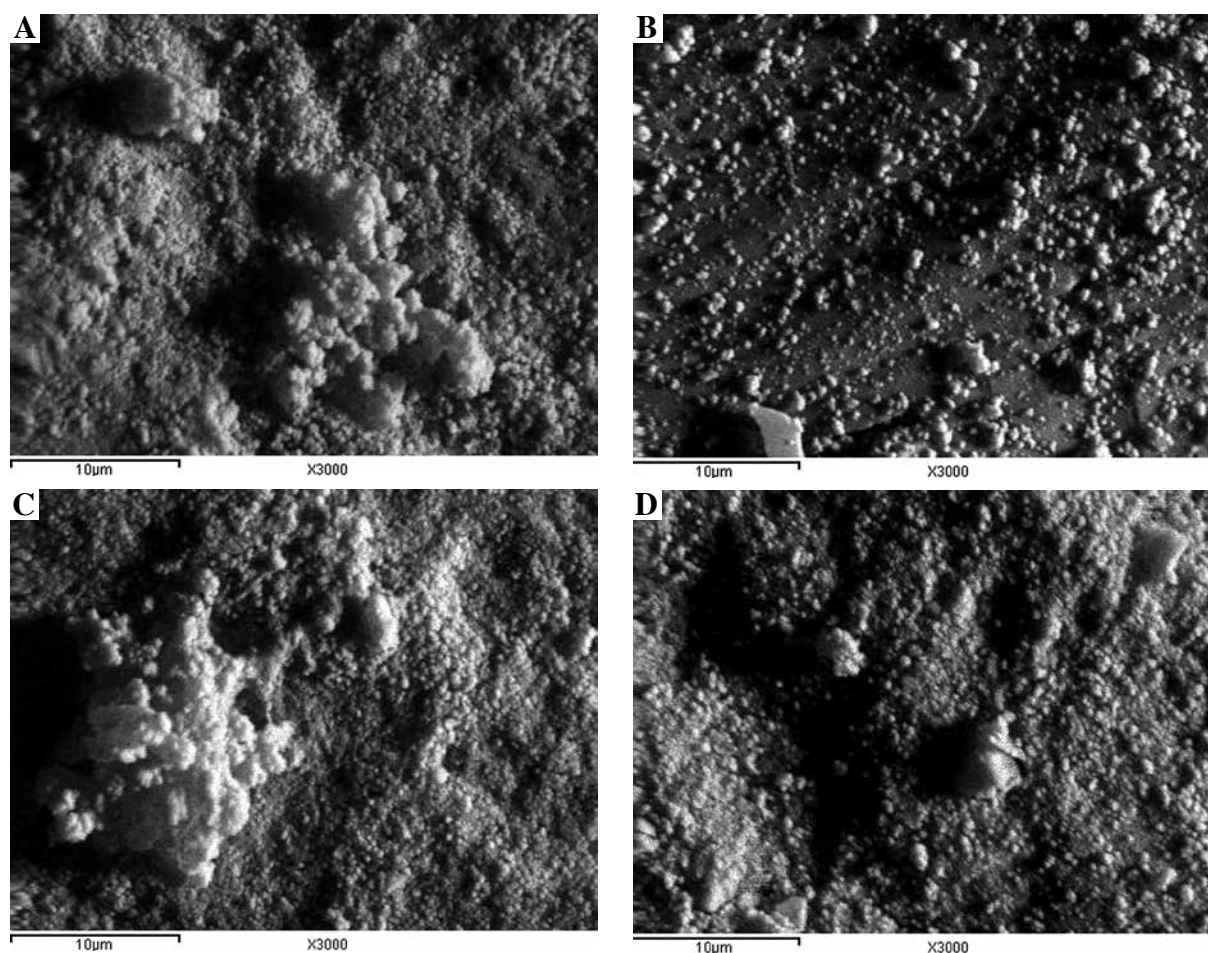


**Fig. 4.** Clearly visible characteristic accumulation of various sizes of spherical particles that covered the surface of pure zirconium (A); particles of  $\text{SiO}_2$ :  $\text{ZrO}_2$  1 : 1 (B); particles of  $\text{SiO}_2$ :  $\text{ZrO}_2$  1 : 2 (C); and particles of  $\text{SiO}_2$ :  $\text{ZrO}_2$  1 : 3 (D)

**Table 2.** Detected bands using ISSR analysis in male mice treated with high dose (400 mg/kg) of  $\text{SiO}_2$ ,  $\text{TiO}_2$ , and  $\text{ZrO}_2$ -Ps

Treatment	Mobility range bp	Total band Nos.	Mean band (X ± SEM)	Mono-morphic	Mono-morphic (%)	Poly-morphic	Poly-morphic (%)
Control	1360-168	90	15.0 ±0.01	84.0	93.3	6	6.7
Cyclophosphamide	1392-112	111	18.5 ±0.02	74.0	66.7	37	33.3
$\text{SiO}_2$	1354-157	92	15.3 ±0.01	79.0	85.9	13	14.1
$\text{TiO}_2$	1387-114	101	16.8 ±0.02	77.0	76.2	24	23.8
$\text{ZrO}_2$	1369-158	94	15.7 ±0.01	82.0	87.2	12	12.8
$\text{SiO}_2$ : $\text{TiO}_2$ (1 : 1)	1372-152	95	15.8 ±0.02	79.0	83.2	16	16.8
$\text{SiO}_2$ : $\text{TiO}_2$ (1 : 2)	1383-135	96	16.0 ±0.01	77.0	80.2	19	19.8
$\text{SiO}_2$ : $\text{TiO}_2$ (1 : 3)	1389-117	99	16.5 ±0.01	75.0	75.8	24	24.2
$\text{SiO}_2$ : $\text{ZrO}_2$ (1 : 1)	1358-156	92	15.3 ±0.01	80.0	87.0	12	13.0
$\text{SiO}_2$ : $\text{ZrO}_2$ (1 : 2)	1372-152	92	15.3 ±0.01	79.0	85.9	13	14.1
$\text{SiO}_2$ : $\text{ZrO}_2$ (1 : 3)	1378-134	95	15.8 ±0.02	78.0	82.1	17	17.9

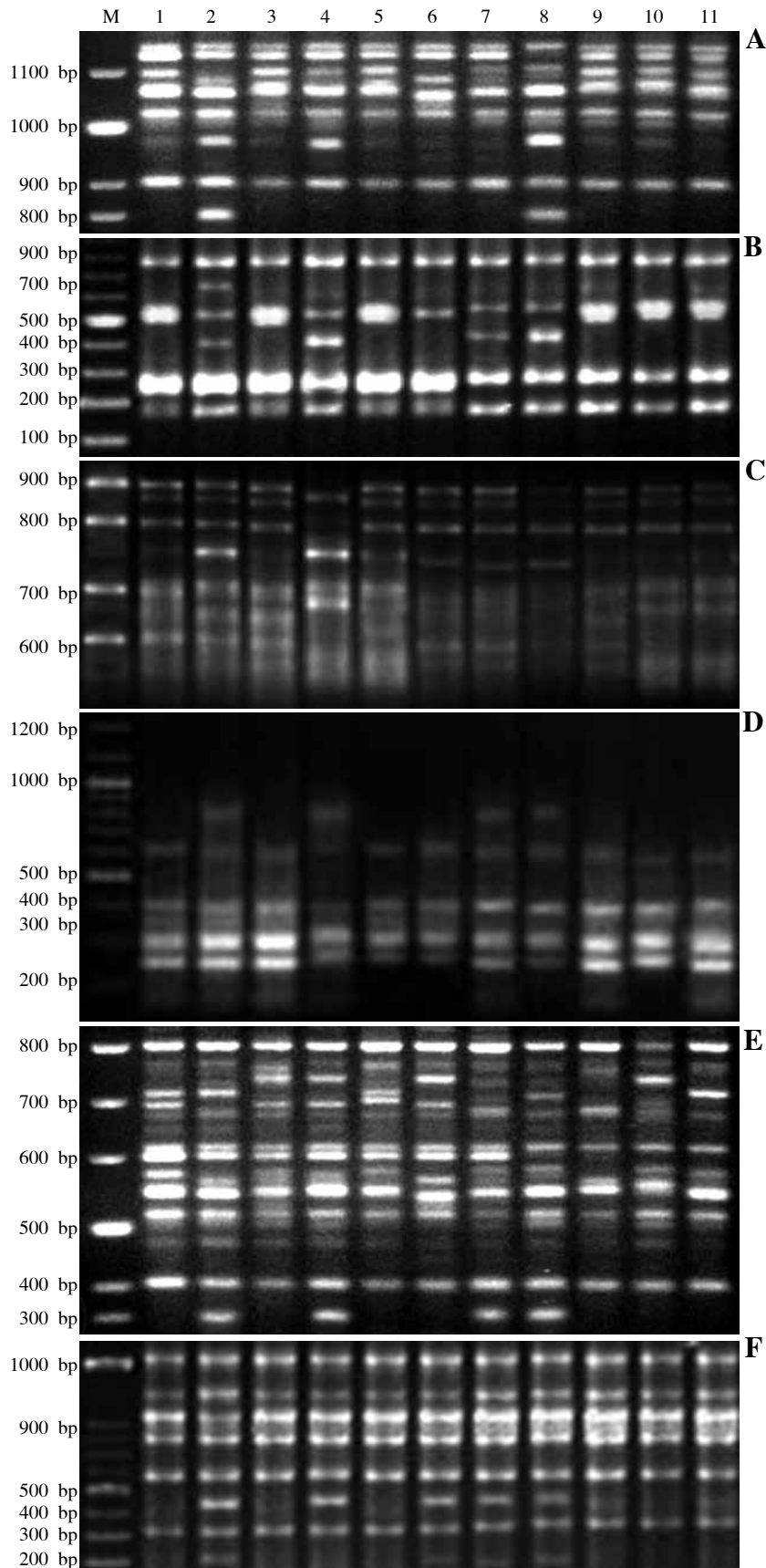


**Fig. 5.** ISSR analysis of mice genome exposed to a high dose (400 mg/kg) of SiO<sub>2</sub>, TiO<sub>2</sub>, and ZrO<sub>2</sub>-Ps using HB8 (A), HB9 (B), HB10 (C), HB11 (D), HB15 (E), and 814 primers. M represents DNA marker; lane 1 represents control mice; lane 2 represents mice treated with cyclophosphamide; lanes 3-5 represent mice treated with SiO<sub>2</sub>, TiO<sub>2</sub>, and ZrO<sub>2</sub>-Ps, respectively; lanes 6-8 represent mice treated with mixture of SiO<sub>2</sub> and TiO<sub>2</sub> as ratio of 1 : 1, 1 : 2, and 1 : 3, respectively; lanes 9-11 represent mice treated with mixture of SiO<sub>2</sub> and ZrO<sub>2</sub> as ratio of 1 : 1, 1 : 2, and 1 : 3, respectively

## **In vivo study**

### **ISSR analysis**

ISSR analysis was carried out in male mice using six anchor primers (HB8, HB9, HB10, HB11, HB15, and 814) to determine the genetic variation induced by treatment with mixed and unmixed SiO<sub>2</sub>, TiO<sub>2</sub>, and ZrO<sub>2</sub>-Ps. The current study revealed no differences observed between untreated mice and those treated with low or medium doses of unmixed and mixed SiO<sub>2</sub>, TiO<sub>2</sub>, and ZrO<sub>2</sub>-Ps. Exceptionally, the highest dose (400 mg/kg b.w.) of unmixed and mixed SiO<sub>2</sub>, TiO<sub>2</sub>, and ZrO<sub>2</sub>-Ps caused significant differences compared with the control mice, as summarised in Fig. 5 and Table 2. Untreated mice revealed the highest percentage of the monomorphic bands (93.3%) and lowest percentage (6.7%) of the polymorphic bands (Table 2). However, the highest percentage of the polymorphic bands was observed in mice treated with CP, TiO<sub>2</sub>, and the mixture 1SiO<sub>2</sub>:3TiO<sub>2</sub> (33.3%, 23.8% and 24.2%, respectively) (Table 2).

### **Micronucleus (MN) assay**

Figure 6 summarises the effect of SiO<sub>2</sub>, TiO<sub>2</sub>, and ZrO<sub>2</sub>-Ps in mixed and unmixed form on MnPCE formation in the bone marrow cells of male mice. The results showed that low and medium doses of mixed and unmixed SiO<sub>2</sub>, TiO<sub>2</sub>, and ZrO<sub>2</sub>-Ps did not increase significantly the incidence of MnPCEs in comparison to the control group (Fig. 6). However, exposure of male mice with high doses of TiO<sub>2</sub>-Ps alone or in combination with SiO<sub>2</sub>-Ps with the ratio of 1 : 1, 2 : 1, and 3 : 1 increased significantly the incidence of MnPCEs (11.6 ± 0.1, 10.9 ± 0.2; 11.5 ± 0.1, and 13.3 ± 0.3, respectively) compared with that of the control group (4.9 ± 0.1, Fig. 6). On the other hand, treatment of male mice with high doses of SiO<sub>2</sub>- and ZrO<sub>2</sub>-Ps alone or in combination with each other with the ratio of 1 : 1, 1 : 2, and 1 : 3 did not increase significantly the MnPCEs formation in the bone marrow cells (Fig. 6).

### **Comet assay in liver tissues**

The genotoxic effect of SiO<sub>2</sub>, TiO<sub>2</sub>, and ZrO<sub>2</sub>-Ps in mixed and unmixed form in male mice is summarised in Table 3. The hepatic tissues of male mice exposed to SiO<sub>2</sub>, TiO<sub>2</sub>, and ZrO<sub>2</sub>-Ps showed considerable dose-dependent DNA damage when estimated by comet assay for DNA strand break in nuclei from individual cells. The results showed that there were no significant differences in the DNA damage values caused by low and medium doses of mixed and unmixed SiO<sub>2</sub>, TiO<sub>2</sub>, and ZrO<sub>2</sub>-Ps and even the control group. Conversely, DNA damaged cells were significantly high in mice exposed to the highest dose of TiO<sub>2</sub>-Ps (19%) and 1 SiO<sub>2</sub>: 3 TiO<sub>2</sub> (20%), compared to control mice (9%) (Table 1). Furthermore, the DNA damaged cells categorised as class 3 were also higher in mice exposed to TiO<sub>2</sub>-Ps and 1SiO<sub>2</sub>: 3TiO<sub>2</sub> than in other groups, except for the group exposed to cyclophosphamide (Table 3).

In addition, the DNA damaged cells in mice exposed to 400 mg/kg of 1SiO<sub>2</sub>: 12TiO<sub>2</sub> and 1SiO<sub>2</sub>: 2TiO<sub>2</sub> were increased but without significant differences (Table 1). On the other hand, other Ps were not able to significantly increase the DNA damage in hepatic cells of male mice, which were relatively similar to those of the control fish.

### **Determination of glutathione peroxidase activity**

Table 4 shows the results of glutathione peroxidase activity after treatment of male mice with mixed and unmixed SiO<sub>2</sub>, TiO<sub>2</sub>, and ZrO<sub>2</sub>-Ps. The present study showed that male mice exposed to mixed or unmixed SiO<sub>2</sub>, TiO<sub>2</sub>, and ZrO<sub>2</sub>-Ps in low and medium doses had relatively similar values to untreated mice (data not shown). However, the values of glutathione peroxidase activity showed significant differences with the treatment of the highest dose of SiO<sub>2</sub>, TiO<sub>2</sub> and ZrO<sub>2</sub>-Ps, where treatment of male mice with TiO<sub>2</sub>-Ps either in unmixed form or mixed form with SiO<sub>2</sub> decreased significantly the values of glutathione peroxidase activity (Table 4). However, other types of the used Ps did not induce significant reduction in the glutathione peroxidase activity with 400 mg/kg, whereas the activity values in mice treated with SiO<sub>2</sub> and ZrO<sub>2</sub>-Ps were similar to those in untreated mice (Table 4).

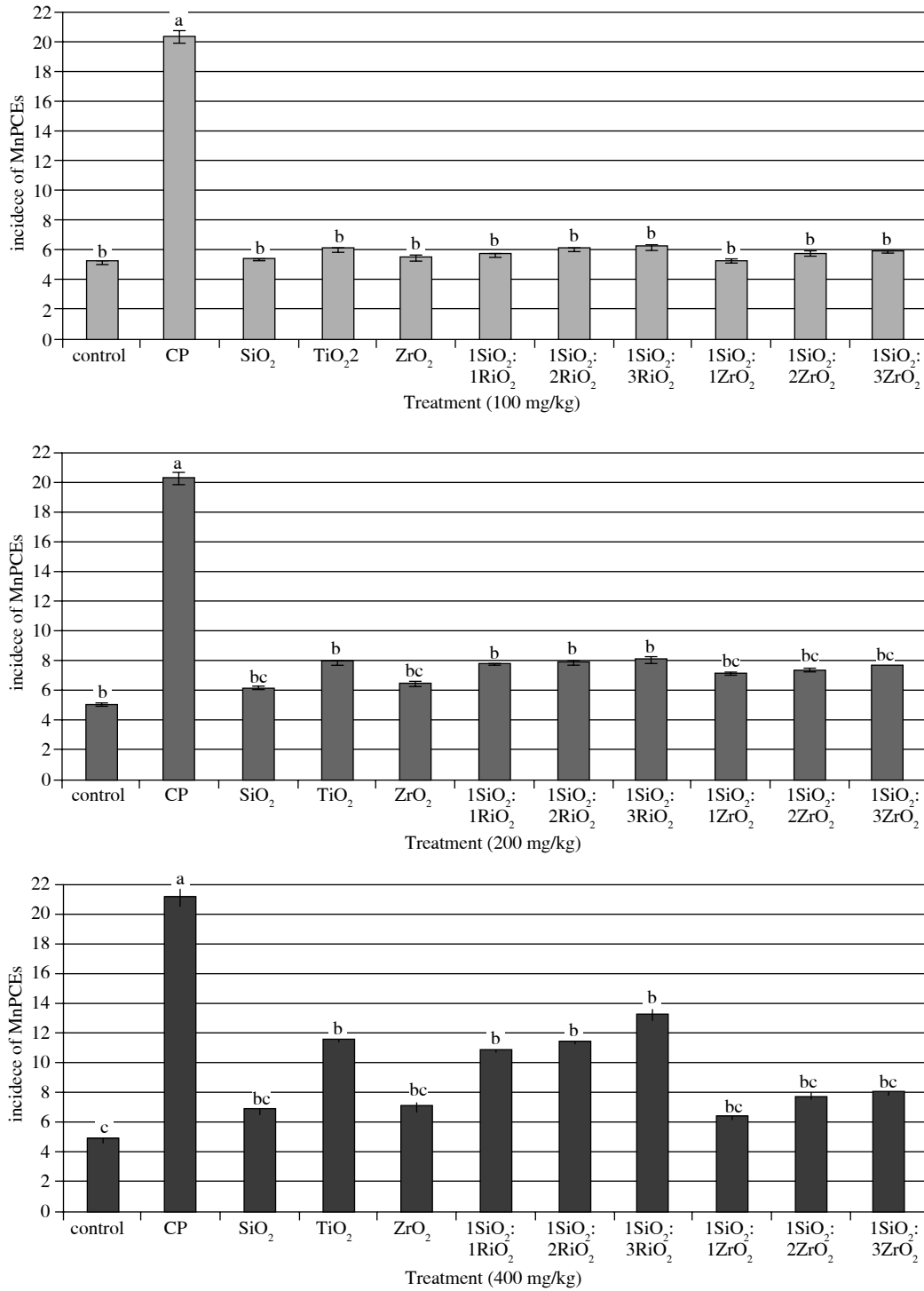
### **Determination of albumin, globulin, and A/G ratio**

Table 5 represents the results of albumin, globulin, and A/G ratio after treatment of male mice with mixed and unmixed SiO<sub>2</sub>, TiO<sub>2</sub>, and ZrO<sub>2</sub>-Ps. The results found that male mice exposed to mixed or unmixed SiO<sub>2</sub>, TiO<sub>2</sub>, and ZrO<sub>2</sub>-Ps in low and medium doses had relatively similar values of albumin, globulin, and A/G to untreated mice (data not shown). In contrast, the values of albumin, globulin, and A/G showed significant differences with the treatment of the highest dose (400 mg/kg) of SiO<sub>2</sub>, TiO<sub>2</sub>, and ZrO<sub>2</sub>-Ps, in which treatment of male mice with TiO<sub>2</sub>-Ps either in unmixed form or mixed form with SiO<sub>2</sub> decreased significantly the levels of albumin and globulin (Table 5). However, other types of used Ps did not prompt significant changes in the levels of albumin and globulin with 400 mg/kg compared with control mice (Table 5).

### **Assessment the population of lymphocytes in peripheral blood**

Figure 7 exemplifies the results of the distribution of lymphocyte population in the peripheral blood of male mice exposed to mixed and unmixed SiO<sub>2</sub>, TiO<sub>2</sub>, and ZrO<sub>2</sub>-Ps. male mice exposed to mixed or unmixed SiO<sub>2</sub>, TiO<sub>2</sub>, and ZrO<sub>2</sub>-Ps in low and medium doses had relatively analogous values to untreated mice (data not shown). At the highest dose of SiO<sub>2</sub>, TiO<sub>2</sub>, and ZrO<sub>2</sub>-Ps the results revealed that no significant differences were found in the distribution of T-cell and NK-cell populations between treated and control animals ( $p > 0.05$ ). However, distribution





CP – cyclophosphamide

**Fig. 6.** Micronucleated polychromatic erythrocytes (MnPCEs) of male mice exposed to different doses of SiO<sub>2</sub>, TiO<sub>2</sub>, and ZrO<sub>2</sub>-Ps. Results are expressed as mean ± SEM of data from at least ten samples. Mean values within tissue with unlike superscript letters were significantly different ( $p < 0.05$ , Scheffé-Test) (A-C). Mean values within tissue with similar superscript letters were not significant differences ( $p > 0.05$ ) (B, C)

**Table 3.** Visual score of DNA damage in male mice exposed to high dose (400 mg/kg) of SiO<sub>2</sub>, TiO<sub>2</sub>, and ZrO<sub>2</sub>-Ps

Treatment	No. of cells		ClassΩ				DNA damaged cells (% mean)
	Analysed	Comet	0	1	2	3	
Control	100	9	91	6	3	0	9c
Cyclophosphamide	100	29	71	8	7	14	29a
SiO <sub>2</sub>	100	10	90	5	4	1	10c
TiO <sub>2</sub>	100	19	81	4	6	9	19b
ZrO <sub>2</sub>	100	11	89	5	3	3	11c
SiO <sub>2</sub> : TiO <sub>2</sub> (1 : 1)	100	12	88	3	5	4	12c
SiO <sub>2</sub> : TiO <sub>2</sub> (1 : 2)	100	15	85	5	4	6	15bc
SiO <sub>2</sub> : TiO <sub>2</sub> (1 : 3)	100	20	80	1	7	12	20b
SiO <sub>2</sub> : ZrO <sub>2</sub> (1 : 1)	100	10	90	4	3	3	10c
SiO <sub>2</sub> : ZrO <sub>2</sub> (1 : 2)	100	12	88	6	2	4	12c
	100	14	86	5	4	5	14bc

Ω; Class 0 = no tail; 1 = tail length < diameter of nucleus; 2 = tail length between 1 × and 2 × the diameter of nucleus; and 3 = tail length > 2 × the diameter of nucleus.

**Table 4.** The amount of glutathione peroxidase activity in mice exposed to SiO<sub>2</sub>, TiO<sub>2</sub>, and ZrO<sub>2</sub> Ps (mg/kg b.w.).

Treatment*	Glutathione peroxidase activity (U/mg tissues/min)		
	100*	200*	400*
Control	5.5 ±0.02 <sup>a</sup>	5.4 ±0.03 <sup>a</sup>	5.7 ±0.01 <sup>a</sup>
Cyclophosphamide	1.7 ±0.05 <sup>b</sup>	1.7 ±0.04 <sup>b</sup>	1.6 ±0.05 <sup>c</sup>
SiO <sub>2</sub>	5.4 ±0.04 <sup>a</sup>	5.1 ±0.05 <sup>a</sup>	4.9 ±0.03 <sup>a</sup>
TiO <sub>2</sub>	5.0 ±0.03 <sup>a</sup>	4.8 ±0.04 <sup>a</sup>	2.7 ±0.04 <sup>b</sup>
ZrO <sub>2</sub>	5.2 ±0.03 <sup>a</sup>	5.1 ±0.04 <sup>a</sup>	4.4 ±0.03 <sup>ab</sup>
SiO <sub>2</sub> : TiO <sub>2</sub> (1 : 1)	5.2 ±0.04 <sup>a</sup>	4.8 ±0.03 <sup>a</sup>	2.9 ±0.02 <sup>b</sup>
SiO <sub>2</sub> : TiO <sub>2</sub> (1 : 2)	4.9 ±0.02 <sup>a</sup>	4.7 ±0.05 <sup>a</sup>	2.6 ±0.03 <sup>b</sup>
SiO <sub>2</sub> : TiO <sub>2</sub> (1 : 3)	4.8 ±0.05 <sup>a</sup>	4.5 ±0.06 <sup>a</sup>	2.3 ±0.02 <sup>b</sup>
SiO <sub>2</sub> : ZrO <sub>2</sub> (1 : 1)	5.2 ±0.05 <sup>a</sup>	5.1 ±0.06 <sup>a</sup>	4.2 ±0.04 <sup>ab</sup>
SiO <sub>2</sub> : ZrO <sub>2</sub> (1 : 2)	5.1 ±0.06 <sup>a</sup>	4.9 ±0.04 <sup>a</sup>	4.1 ±0.05 <sup>ab</sup>
SiO <sub>2</sub> : ZrO <sub>2</sub> (1 : 3)	5.0 ±0.04 <sup>a</sup>	4.8 ±0.06 <sup>a</sup>	4.0 ±0.02 <sup>ab</sup>

\*Each treatment had an equivalent numbers of animals (n = 10)

<sup>a,b,c</sup>Mean values within tissue with unlike superscript letters were significantly different (p < 0.05, Scheffé-Test)

<sup>a,b,ab</sup>Mean values within tissue with similar superscript letters were not significant differences (p > 0.05)

of B-cell population was increased significantly (p < 0.05) with TiO<sub>2</sub> treatment either in mixed or unmixed forms.

#### Determination of ALT and AST

Table 6 represents the parameters of liver function (ALT and AST) after treatment of male mice with both mixed and unmixed SiO<sub>2</sub>, TiO<sub>2</sub>, and ZrO<sub>2</sub>-Ps. The results showed that mice exposed to mixed or unmixed SiO<sub>2</sub>, TiO<sub>2</sub>, and ZrO<sub>2</sub>-Ps in low and medium doses had values of ALT and AST relatively comparable to control mice (data not shown). However, the values of ALT and AST showed significant

variance with the treatment of the highest dose (400 mg/kg) of SiO<sub>2</sub>, TiO<sub>2</sub>, and ZrO<sub>2</sub>-Ps, in which treatment of mice with TiO<sub>2</sub>-Ps either in unmixed form or mixed form with SiO<sub>2</sub> increased significantly the levels of ALT and AST (Table 6). However, other types of the used Ps did not give significant changes in the levels of ALT and AST with 400 mg/kg compared with control mice (Table 5).

#### Discussion

Although great developments have been made in the worldwide production and use of metal-based composites

**Table 5.** Levels of Albumin, globulin, and A/G ratio in serum of male mice exposed to SiO<sub>2</sub>, TiO<sub>2</sub>, and ZrO<sub>2</sub>-Ps (mg/kg b.w.)

Treatment*	Particulars		
	Albumin	Globulin	A/G ratio
Control	5.7 ±0.3 <sup>a</sup>	3.2 ±0.1 <sup>a</sup>	1.26 ±0.2 <sup>b</sup>
Cyclophosphamide	2.3 ±0.4 <sup>b</sup>	1.8 ±0.2 <sup>b</sup>	1.54 ±0.3 <sup>ab</sup>
SiO <sub>2</sub>	4.9 ±0.2 <sup>a</sup>	3.0 ±0.3 <sup>a</sup>	1.32 ±0.2 <sup>a</sup>
TiO <sub>2</sub>	3.2 ±0.3 <sup>ab</sup>	2.3 ±0.4 <sup>ab</sup>	1.68 ±0.1 <sup>a</sup>
ZrO <sub>2</sub>	4.6 ±0.5 <sup>a</sup>	2.8 ±0.3 <sup>a</sup>	1.42 ±0.4 <sup>ab</sup>
SiO <sub>2</sub> : TiO <sub>2</sub> (1 : 1)	4.3 ±0.3 <sup>a</sup>	2.7 ±0.2 <sup>a</sup>	1.48 ±0.2 <sup>ab</sup>
SiO <sub>2</sub> : TiO <sub>2</sub> (1 : 2)	3.9 ±0.1 <sup>ab</sup>	2.5 ±0.1 <sup>a</sup>	1.84 ±0.2 <sup>a</sup>
SiO <sub>2</sub> : TiO <sub>2</sub> (1 : 3)	3.1 ±0.4 <sup>ab</sup>	2.0 ±0.3 <sup>b</sup>	1.96 ±0.3 <sup>a</sup>
SiO <sub>2</sub> : ZrO <sub>2</sub> (1 : 1)	4.6 ±0.6 <sup>a</sup>	2.9 ±0.4 <sup>a</sup>	1.33 ±0.1 <sup>ab</sup>
SiO <sub>2</sub> : ZrO <sub>2</sub> (1 : 2)	4.1 ±0.5 <sup>a</sup>	2.6 ±0.2 <sup>ab</sup>	1.38 ±0.3 <sup>ab</sup>
SiO <sub>2</sub> : ZrO <sub>2</sub> (1 : 3)	3.8 ±0.3 <sup>ab</sup>	2.4 ±0.1 <sup>ab</sup>	1.41 ±0.1 <sup>ab</sup>

<sup>a,b,c</sup>Mean values within tissue with unlike superscript letters were significantly different ( $p < 0.05$ , Scheffé-Test)  
<sup>a,b,ab</sup>Mean values within tissue with similar superscript letters were not significant differences ( $p > 0.05$ )

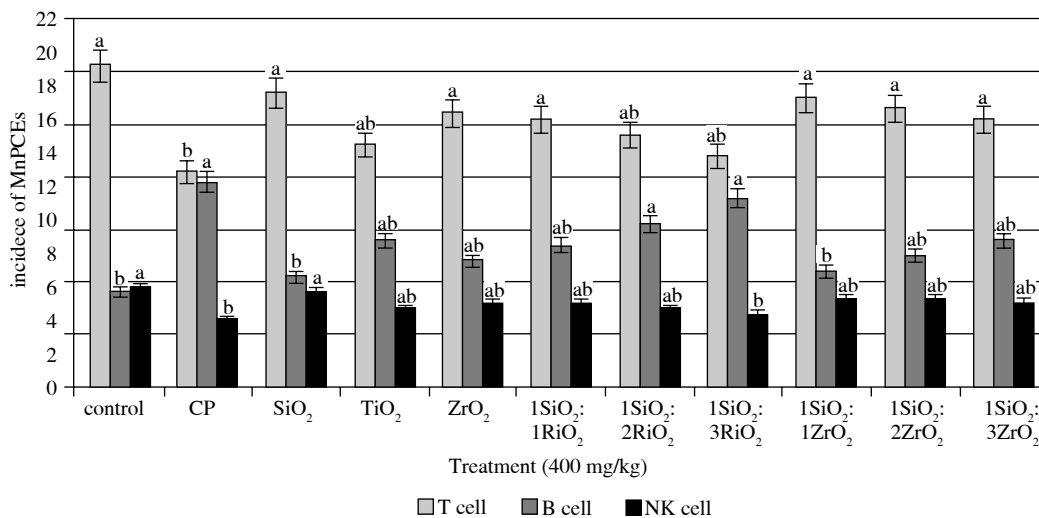


**Fig. 7.** Population of lymphocyte distribution of peripheral blood from male mice exposed to different doses of SiO<sub>2</sub>, TiO<sub>2</sub>, and ZrO<sub>2</sub>-Ps

and nanoparticles, there is a serious lack of information about the impact of these materials on human health and environment, especially the potential for induced toxicity [44]. Preliminary reports of the inherent toxicity of some metals nanoparticles (NPs) are available and indicate that they can affect biological behaviour at the organ, tissue, cellular, subcellular, and protein levels.

Schrand *et al.* [45] reported that as particle size decreases, some metal-based NPs showed increment in their toxicity. NPs also interact with proteins and enzymes within mammalian cells and interfere with the antioxidant defence mechanism leading to reactive oxygen species

generation, the initiation of an inflammatory response, and perturbation and destruction of the mitochondria causing apoptosis or necrosis. Therefore, the main objective of the current study was to use larger particles than nanoparticles to decrease the risk of the potential toxicity attributed to the use of small particles of materials under study.

The present work showed that the treatment of male mice with SiO<sub>2</sub> and ZrO<sub>2</sub> in separate or in mixture form exhibited lower toxicity values than those resulting from TiO<sub>2</sub>. Furthermore, the present study demonstrated that 100 and 200 mg/kg b.w. of SiO<sub>2</sub>, TiO<sub>2</sub>, and ZrO<sub>2</sub>-Ps in ei-

**Table 6.** Levels of hepatic factors in male mice exposed to high dose (400 mg/kg) of SiO<sub>2</sub>, TiO<sub>2</sub>, and ZrO<sub>2</sub> Ps

Treatment*	Hepatic factors	
	ALT (U/l)	AST (U/l)
Control	23 ±1.2 <sup>b</sup>	72 ±4.2 <sup>c</sup>
Cyclophosphamide	42 ±2.7 <sup>a</sup>	173 ±4.2 <sup>a</sup>
SiO <sub>2</sub>	26 ±1.4 <sup>b</sup>	81 ±2.5 <sup>c</sup>
TiO <sub>2</sub>	34 ±1.6 <sup>ab</sup>	142 ±3.4 <sup>b</sup>
ZrO <sub>2</sub>	28 ±2.3 <sup>ab</sup>	83 ±3.1 <sup>c</sup>
SiO <sub>2</sub> : TiO <sub>2</sub> (1 : 1)	29 ±2.2 <sup>ab</sup>	121 ±4.1 <sup>b</sup>
SiO <sub>2</sub> : TiO <sub>2</sub> (1 : 2)	33 ±1.9 <sup>ab</sup>	138 ±3.4 <sup>b</sup>
SiO <sub>2</sub> : TiO <sub>2</sub> (1 : 3)	38 ±3.1 <sup>a</sup>	149 ±4.5 <sup>b</sup>
SiO <sub>2</sub> : ZrO <sub>2</sub> (1 : 1)	24 ±2.1 <sup>b</sup>	79 ±1.1 <sup>c</sup>
SiO <sub>2</sub> : ZrO <sub>2</sub> (1 : 2)	27 ±2.4 <sup>ab</sup>	87 ±2.9 <sup>c</sup>
SiO <sub>2</sub> : ZrO <sub>2</sub> (1 : 3)	30 ±2.7 <sup>ab</sup>	89 ±2.4 <sup>c</sup>

<sup>a,b,c</sup>Mean values within tissue with unlike superscript letters were significantly different ( $p < 0.05$ , Scheffé-Test)

<sup>a,b,ab</sup>Mean values within tissue with similar superscript letters were not significant differences ( $p > 0.05$ )

ther mixed or unmixed form were safe in male mice using several genotoxicity and biochemical assays. However, using 400 mg/kg of TiO<sub>2</sub>-Ps in unmixed form or mixed with SiO<sub>2</sub> increased the toxicity potential using ISSR analysis, micronucleus test, comet assay, and glutathione peroxidase activity. In good agreement with our work, Heckmann *et al.* [46] reported that TiO<sub>2</sub> particles were the only metal that initiated toxic effects to earthworms compared with other metals, such as Ag, Cu, Ni, Al<sub>2</sub>O<sub>3</sub>, SiO<sub>2</sub>, and ZrO<sub>2</sub> particles. In addition, TiO<sub>2</sub>-NP has previously been reported to induce toxicity to bacteria [47] and the freshwater crustacean *Daphnia magna* [48].

Conversely, a recent study by Lindberg *et al.* [49] demonstrated that inhalation of mice with nano-sized TiO<sub>2</sub> (74% anatase, 26% brookite; five days, four hours/day) resulted in a clear increase in neutrophils in BAL (mouse bronchoalveolar lavage) fluid, indicating an inflammatory effect; however, no significant effect on the level of DNA damage in lung epithelial cells or micronuclei in PCEs was observed. They suggested that inhalation exposure resulted in much lower systemic TiO<sub>2</sub> doses than the IP injection and intraperitoneal treatments. Therefore, the lung epithelial cells probably received considerably less TiO<sub>2</sub> than BAL cells. These findings support our results, in which the mice in the present experiment were treated IP and consequently had greater toxicity than inhalation exposure. Another recent study by Sadiq *et al.* [50] reported that TiO<sub>2</sub> can reach the mouse bone marrow and is prone to inducing cytotoxicity. These results were obtained when mice were treated intravenously with three daily doses of 50 mg/kg TiO<sub>2</sub> NPs.

These results demonstrate that nanoparticles of TiO<sub>2</sub> can potentially cause adverse effects on organ, tissue, cellular, subcellular, and protein levels due to their unusual physicochemical properties, such as small size [45]. However, our study found that genotoxicity of TiO<sub>2</sub> was observed only with the highest dose (400 mg/kg) of TiO<sub>2</sub> particles; treatment of male mice in the current study with 100 or 200 mg/kg of TiO<sub>2</sub> particles did not cause any genotoxicity symptoms. These results suggest that as particle size decreases, some metals show increased toxicity, even if the same material is relatively inert in its bulk form [45].

Moreover, an explanation for the mechanism thought to be responsible for the genetic alterations exerted by TiO<sub>2</sub> involves oxidative stress, in which several studies showed that TiO<sub>2</sub> induced reactive oxygen species (ROS) in a variety of cell types and tissues [51-56]. Our results are in a good settlement with these findings, where TiO<sub>2</sub> inhibits the antioxidant activity of the glutathione peroxidase enzyme. It is increasingly proposed that ROS and reactive nitrogen species (RNS) play a vital role in DNA damage and cancer development [57, 58].

Reactive oxygen species is a collective term often used by biologists to include oxygen radicals [superoxide (O<sub>2</sub><sup>-</sup>), hydroxyl (OH), peroxy (RO<sub>2</sub>), and alkoxy (RO)] and certain nonradicals that are either oxidising agents and/or are easily converted into radicals, such as HOCl, ozone (O<sub>3</sub>), peroxyntirite (ONOO<sup>-</sup>), singlet oxygen (<sup>1</sup>O<sub>2</sub>), and H<sub>2</sub>O<sub>2</sub>. The mechanism of ROS inducing DNA damage could be attributed to one or more reasons as follows: (1) ROS causes structural alterations in DNA, e.g. base pair mutations, rearrangements, deletions, insertions, and sequence amplification [58]; (2) affect cytoplasmic and nuclear signal transduction pathways [59, 58]; and (3) modulate the activity of the proteins and genes that respond to stress and act to regulate the genes that are related to cell proliferation, differentiation, and apoptosis [59, 58].

The immune organs and cells play a vigorous role during the body defence progress for xenobiotics. The present study revealed that treatment of male mice with TiO<sub>2</sub>-Ps either in mixed or unmixed forms of SiO<sub>2</sub> decreased significantly the levels of albumin and globulin and increased the B-cell population as well as ALT and AST in the mice samples. In agreement with our findings, in mice treated with nano-TiO<sub>2</sub>, their liver showed congestion and other diseases, as well as decreased levels of albumin, globulin and levels of leucocytes and T cells, glutamate aminotransferase, and AST, which are all related to liver function. These results indicate that TiO<sub>2</sub> impairs the immunity of the liver and alters liver function [60]. In addition, Li *et al.* reported that exposure to TiO<sub>2</sub> by intraperitoneal injection induced obvious congestion and lymph nodule proliferation in the mouse spleen [61]. These results indicated that exposure to TiO<sub>2</sub> particles could translocate throughout the body quickly and tend to accumulate in immune organs, possibly through uptake by migratory antigen presenting cells, because many

toxicological studies have observed that macrophages or foreign-body giant cells appeared in lung tissue as exposure doses increased [62].

In conclusion, the current study found that TiO<sub>2</sub> composite induced *in vivo* immune and genetic toxicity in a dose-dependent manner in mice. However, SiO<sub>2</sub>, and ZrO<sub>2</sub> composites revealed a lower toxicity in male mice compared to TiO<sub>2</sub>. These data suggest that SiO<sub>2</sub> and ZrO<sub>2</sub> composites expressed a low toxicity rate and could be used in biomedical applications such as repair bone defects. Moreover, we should be concerned about the potential risk of cancer or genetic disorders especially for people occupationally exposed to high concentrations of TiO<sub>2</sub>, and that it might be prudent to limit ingestion of TiO<sub>2</sub> through nonessential drug additives, food colourings, etc.

*The project was supported by King Saud University, Deanship of Scientific Research, College of Science and Research Centre.*

*The authors declare no conflicts of interest.*

## References

- Hench LL (1991): Bioceramics: from concept to clinic. *J Am Ceram Soc* 74: 1487-1510.
- LeGeros RZ, LeGeros JP: Dense hydroxyapatite. In: An introduction to bioceramics. Hench LL, Wilson J (eds.). Singapore, World Scientific. 1993; 139-180.
- Gross UM, Muller-Mai C, Voigt C: Ceravital bioactive ceramics. In: An introduction to bioceramics. Hench LL, Wilson J (eds.). Singapore, World Scientific. 1993; 105-124.
- Kokubo T, Shigematsu M, Nagashima Y, et al. (1982): Apatite and wollastonite-containing glass-ceramics for prosthetic application. *Bull Inst Chem Res Kyoto Univ* 60: 260-268.
- Kokubo T: A/W glass-ceramics: processing and properties. In: An introduction to bioceramics. Hench LL, Wilson J (eds.). Singapore, World Scientific. 1993; 75-88.
- Kokubo T (1991): Bioactive glass ceramics: properties and applications. *Biomaterials* 12: 155-163.
- Kokubo T, Ito S, Huang ZT, et al. (1990): Ca, P-rich layer formed on high-strength bioactive glass-ceramic A-W. *J Biomed Mater Res* 24: 331-343.
- Kokubo T, Kushitani H, Sakka S, et al. (1990): Solutions able to reproduce *in vivo* surface-structure changes in bioactive glass-ceramic A-W. *J Biomed Mater Res* 24: 721-734.
- Cho SB, Nakanishi K, Kokubo T, et al. (1995): Dependence of apatite formation on silica gel on its structure: effect of heat treatment. *J Am Ceram Soc* 78: 1769-1774.
- Kokubo T, Takadama H (2006): How useful is SBF in predicting *in vivo* bone bioactivity? *Biomaterials* 27: 2907-2915.
- Ohtsuki C, Kamitakahara M, Miyazaki T (2009): Bioactive ceramic-based materials with designed reactivity for bone tissue regeneration. *J R Soc Interface* 6: S349-S360.
- Zhang YH, Reller A (2003): Investigation of mesoporous and microporous nanocrystalline silicon doped titania. *Materials Letters* 57: 4108-4113.
- Jiang XC, Herricks T, Xia YN (2003): One-dimensional nanostructures: synthesis, characterization and applications. *Adv Mater* 15: 1205-1209.
- Haugen H, Will J, Kohler A, et al. (2004): Ceramic TiO<sub>2</sub>-foams: characterization of a potential scaffold. *J Eur Ceram Soc* 24: 661-668.
- Meretoja VV, Tirri T, Aaritalo V, et al. (2007): Titania and titania-silica coatings for titanium: comparison of ectopic bone formation within cell-seeded scaffolds. *Tissue Eng* 13: 855-863.
- Wu JM, Liu JF, Hayakawa S, et al. (2007): Low-temperature deposition of rutile film on biomaterials substrates and its ability to induce apatite deposition *in vitro*. *J Mater Sci Mater Med* 18: 1529-1536.
- Hong SS, Lee MS, Park SS, et al. (2003): Synthesis of nano-sized TiO<sub>2</sub>/SiO<sub>2</sub> particles in the microemulsion and their photocatalytic activity on the decomposition of p-nitrophenol. *Catal Today* 87: 99-105.
- Soo WL, Morillo C, Lira-Olivares J, et al. (2003): Tribological and microstructural analysis of Al<sub>2</sub>O<sub>3</sub>/TiO<sub>2</sub> nanocomposites to use in the femoral head of hip replacement. *Wear* 255: 1040-1044.
- Li J, Hastings GW: In: *Handbook of Biomaterial Properties*. Black J, Hastings GW (eds.). Chapman and Hall, London, New York. 1998; 340.
- Burger W, Richter HG, Piconi C, et al. (1997): New Y-TZP powders for medical grade zirconia. *J Mater Sci Mater Med* 8: 113-118.
- Liang H, Huang Y, He F, et al. (2007): Enhanced calcium phosphate precipitation on the surface of Mg-Ion-implanted ZrO<sub>2</sub> bioceramic. *Surf Rev Lett* 14: 71-77.
- Cales B (2000): Zirconia as a sliding material. *Clin Orthop Relat Res* 379: 94-112.
- Clarke IC, Manaka M, Green DD, et al. (2003): Current status of zirconia used in total hip implants. *J Bone Joint Surg Am* 85: 73-84.
- Kosmac T, Oblak C, Jevnikar P, et al. (2000): Strength and reliability of surface treated Y-TZP dental ceramics. *J Biomed Mater Res* 53: 304-313.
- Benzaid R, Chevalier J, Malika Saadaoui M, et al. (2008): Fracture toughness, strength and slow crack growth in a ceria stabilized zirconia-alumina nanocomposite for medical applications. *Biomaterials* 29: 3636-3641.
- Uchida M, Kim HM, Kokubo T, et al. (2002): Apatite forming ability of a Zirconia/ Alumina nano composite induced by chemical treatment. *J Biomed Mater Res* 60: 277-282.
- Sharif MA, Sueyoshi H (2008): Microstructure and Properties of Wet Mixed Pyrolyzed ZrO<sub>2</sub>/Si/Phenol Resin Composite. *Synth React Inorg Met Org Chem* 38: 194-200.
- Yan YY, Lu C (2009): Ultraviolet enhanced bioactivity of zirconia films prepared by micro-arc oxidation. *Thin Solid Films* 517: 1577-1581.
- Ohtsuki C, Iida H, Nakamura S, et al. (1997): Bioactivity of titanium treated with hydrogen peroxide solutions containing metal chlorides. *J Biomed Mater Res* 35: 39-47.
- Velmurugan R, Kanagesan S, Jesurani S, et al. (2010): Surface Bioactivity of Sol Gel Derived 3Y-TZP Bioinert Ceramic through Hydroxylation Technique using 5M NaOH. *Eur J Sci Res* 41: 430-436.
- Najda J, Goss M, Gmiński J, et al. (1994): The antioxidant enzymes activity in the conditions of systemic hypersilicemia. *Biol Trace Elem Res* 42: 63-70.
- Asahida T, Kobayashi T, Saitoh K, et al. (1996): Nakayama I. Tissue preservation and total DNA extraction from fish stored at ambient temperature using buffers containing high concentration of urea. *Fish Sci* 62: 727-730.

33. Ueda T, Hayashi M, Koide N, et al. (1992): A preliminary study of the micronucleus test by acridine orange fluorescent staining compared with chromosomal aberration test using fish erythropoietic and embryonic cells. *Water Sci Technol* 25: 235-240.
34. Fairbairn DW, Olive PL, O'Neill KL (1995): Comet assay: A comprehensive review. *Mutat Res* 339: 37-59.
35. Collins A, Dusinska M, Franklin (1997): Comet assay in human biomonitoring studies: Reliability, validation, and applications. *Environ Mol Mutagen* 30: 139-146.
36. El-Megeed GA, Khalil WKB, Abdel Raouf A, et al. (2008): Synthesis and in vivo anti-mutagenic activity of novel melatonin derivatives. *Eur J Med Chem* 43: 763-770.
37. Zárbynická L, Vávrová J, Havelek R, et al. (2013): Lymphocyte subsets and their H2AX phosphorylation in response to in vivo irradiation in rats. *Int J Radiat Biol* 89: 110-117.
38. Rasmy GE, Khalil WKB, Moharib SA, et al. (2011): Dietary fish oil modulates the effect of dimethylhydrazine-induced colon cancer in rats. *Grasas y Aceites* 62: 253-267.
39. SAS (1982): SAS user's guide: statistics, edn. SAS Institute Inc., Cary, NC.
40. Karlsson KH (2004): Bioactivity of glass and bioactive glasses for bone repair. *Glass Technology* 45: 157-161.
41. Ebisawa Y, Kokubo T, Ohura K, et al. (1990): Bioactivity of CaO•SiO<sub>2</sub>-based glasses: in vitro evaluation. *J Mater Sci: Mater Med* 1: 239-244.
42. Beherei HH, Mohamed KR, El-Bassyouni GT (2009): Fabrication and characterization of bioactive glass (45S5)/titanium Biocomposites. *Ceramics International* 35: 1991-1997.
43. Gerhardt LC, Jell GMR, Boccaccini AR (2007): Titanium dioxide (TiO<sub>2</sub>) nanoparticles filled poly (D,L lactid acid) (PDL-LA) matrix composites for bone tissue engineering. *J Mater Sci: Mater Med* 18:1287-1298.
44. Canesi L, Ciacci C, Betti M, et al. (2008): Immunotoxicity of carbon black nanoparticles to blue mussel hemocytes. *Environ Int* 34: 1114.
45. Schrand AM, Rahman MF, Hussain SM, et al. (2010): Metal-based nanoparticles and their toxicity assessment. *Wiley Interdiscip Rev Nanomed Nanobiotechnol* 2(5): 544-68.
46. Heckmann LH, Hovgaard MB, Sutherland DS, et al. (2011): Limit-test toxicity screening of selected inorganic nanoparticles to the earthworm *Eisenia fetida*. *Ecotoxicology* 20: 226-233.
47. Adams LK, Lyon DY, Alvarez PJJ (2006): Comparative eco-toxicity of nanoscale TiO<sub>2</sub>, SiO<sub>2</sub>, and ZnO water suspensions. *Water Res* 40: 3527-3532.
48. Lovern SB, Klaper R (2006): *Daphnia magna* mortality when exposed to titanium dioxide and fullerene (C-60) nanoparticles. *Environ Toxicol Chem* 25:1132-1137.
49. Lindberg HK, Falck GCM, Catalán J, et al. (2012): Genotoxicity of inhaled nanosized TiO<sub>2</sub> in mice. *Mutat Res* 745: 58-64.
50. Sadiq R, Bhalli JA, Yan J, et al. (2012): Genotoxicity of TiO<sub>2</sub> anatase nanoparticles in B6C3F1 male mice evaluated using Pig-a and flow cytometric micronucleus assays. *Mutat Res* 745: 65-72.
51. Warheit DB, Webb TR, Sayes CM, et al. (2006): Pulmonary instillation studies with nanoscale TiO<sub>2</sub> rods and dots in rats: toxicity is not dependent upon particle size and surface area. *Toxicol Sci* 91: 227-236.
52. Grassian VH, O'shaughnessy PT, Adamcakova-Dodd A, et al. (2007): Inhalation exposure study of titanium dioxide nanoparticles with a primary particle size of 2 to 5 nm. *Environ Health Perspect* 115: 397-402.
53. Sayes CM, Wahi R, Kurian PA, et al. (2006): Correlating nanoscale titania structure with toxicity: a cytotoxicity and inflammatory response study with human dermal fibroblasts and human lung epithelial cells. *Toxicol Sci* 92: 174-185.
54. Gurr JR, Wang AS, Chen CH, et al. (2005): Ultrafine titanium dioxide particles in the absence of photoactivation can induce oxidative damage to human bronchial epithelial cells. *Toxicology* 213: 66-73.
55. Long TC, Saleh N, Tilton RD, et al. (2006): Titanium dioxide (P25) produces reactive oxygen species in immortalized brain microglia (BV2): implications for nanoparticle neurotoxicity. *Environ Sci Technol* 40: 4346-4352.
56. Braydich-Stolle LK, Schaeublin NM, Murdock RC, et al. (2009): Crystal structure mediates mode of cell death in TiO<sub>2</sub> nanotoxicity. *J Nanopart Res* 11: 1361-1374.
57. Feig DI, Reid TM, Loeb LA (1994): Reactive oxygen species in tumorigenesis. *Cancer Res* 54: 1890s-1894s.
58. Trouiller B, Reliene R, Westbrook A, et al. (2009): Titanium dioxide nanoparticles induce DNA damage and genetic instability in vivo in mice. *Cancer Res* 69: 8784-8789.
59. Burdon RH (1995): Superoxide and hydrogen peroxide in relation to mammalian cell proliferation. *Free Radic Biol Med* 18: 775-794.
60. Duan Y, Liu J, Ma L, et al (2010): Toxicological characteristics of nanoparticulate anatase titanium dioxide in mice. *Biomaterials* 31: 894-899.
61. Li N, Duan Y, Hong M, et al. (2010): Spleen injury and apoptotic pathway in mice caused by titanium dioxide nanoparticles. *Toxicol Lett* 195: 161-168.
62. Eydner M, Schaudien D, Creutzenberg O, et al. (2012): Impacts after inhalation of nano- and fine-sized titanium dioxide particles: Morphological changes, translocation within the rat lung, and evaluation of particle deposition using the relative deposition index. *Inhal Toxicol* 24: 557-569.